Supplementary Information, belonging to the manuscript:

Orange Carotenoid Protein as a control element in an antenna system based on a DNA nanostructure

Alessio Andreoni*[1,2§], Su Lin[1,5], Haijun Liu[3,4], Robert E. Blankenship[3,4], Hao Yan[2,5], Neal W. Woodbury*[1,5]

[1]Biodesign Center for Innovations in Medicine, The Biodesign Institute, Arizona State University, Tempe, Arizona, United States of America

[2]Biodesign Center for Molecular Design and Biomimetics, The Biodesign Institute, Arizona State University, Tempe, Arizona, United States of America

[3]Department of Biology, Washington University in St. Louis, St. Louis, Missouri, United States of America

[4]Department of Chemistry, Washington University in St. Louis, St. Louis, Missouri, United States of America

[5]School of Molecular Sciences, Arizona State University, Tempe, Arizona, United States of America

[§]Current Affiliation: National Heart, Lung and Blood Institute, National Institutes of Health, Bethesda, Maryland, United States of America

Table of Contents

Materials and Methods

Reagents

The OCP was purified as previously described.[1] The cloning from *Synechocystis* and over-expression in *E. coli* of the FRP will be reported in a separate communication. HEPES buffer, Tween20 were purchased from Sigma-Aldrich. Oligonucleotides were purchased from IDT DNA: unlabeled single stranded DNA was purified by means of polyacrylamide gel electrophoresis (PAGE), dye-modified DNA was provided by the company purified by HPLC. A list of all the strands, with their sequence and modifications, used in this work is presented in Table S1.

Protein to DNA conjugation

The strand St1 was attached to OCP on a cysteine residue by using the following procedure: the strand St1 was first incubated with a 20x molar excess of TCEP to remove the capping molecule that protects the thiol group. The TCEP and the thiol-protective molecule were removed from the solution by using a desalting step on a NAP 10 column. A 100-fold molar excess of *bis*-maleimidoethane (BMOE) was added to the DNA solution and incubated for 1 hours at room temperature. The excess of unreacted linker was removed by precipitating the DNA with 70% ethanol, and subsequently washing the pellet with 70% ethanol to remove the remaining excess of BMOE. The DNA-BMOE precipitated pellet was then dissolved, quantified, and added to an OCP solution in a 5 to 1, DNA to protein, excess. The buffer for the reaction was HEPES 20 mM, pH 7.8, containing 500 mM NaCl. The sample was incubated in the dark at room temperature overnight.

Purification of Protein-St1 conjugate

After overnight incubation, the DNA-protein reaction sample was subject to a buffer exchange to Tris 40 mM , pH 7.2, Tween 20 0.001%. The sample was loaded onto a MonoQ anion exchange column equilibrated with the same buffer and eluted with a gradient of NaCl. By monitoring the UV/Vis absorbance at 260 and 495 nm during the chromatographic run, the peak containing OCP and DNA was identified and collected. Characterization of the protein-DNA conjugate was performed by UV/Vis spectroscopy and by PAGE analysis.

Annealing and purification of the 3arm DNA junction and OCP-3arm

The 3arm DNA junction was annealed by mixing stoichiometric quantities of the strands St1, St2, and St3. In the case of the OCP3arm construct, the OCP-St1 conjugate was used instead of St1. For annealing, the buffer composition was: HEPES 20 mM, pH 7.5, $MgCl_2$ 20 mM, NaCl 150 mM, EDTA 1 mM, Tween 20 0.001%. For simplicity this will be referred to as “OCP3arm buffer”. To anneal the strands a thermal ramp was used: samples were heated to 35 ºC and cooled down to 10 ºC in 2 hours in a PCR setup. The samples were then purified by using size exclusion chromatography to remove the unassembled DNA strands. The purification was performed on a Superdex 200 Increase 10/300 GL (GE Healthcare) equilibrated with OCP3arm buffer.

UV/Vis and Fluorescence Spectroscopy

UV/Vis Spectra were recorded on a Cary50 Bio, or on a Jasco 670 spectrophotometer. To calculate the concentration of the proteins and dyes the following extinction coefficients were

used: 132 $mM^{-1}cm^{-1}$ for OCP at 495 nm, 150 $mM^{-1}cm^{-1}$ for Cy3 at 550 nm, 250 $mM^{-1}cm^{-1}$ for Cy5 at 650 nm, and 13.98 $mM^{-1}cm^{-1}$ for FRP at 280 nm. Illumination of OCP to achieve conversion of the orange form to the red form was achieved by using a Fiber Lite MH 100 light source, passed through a custom made 430/100 nm bandpass filter, and focused on a 1.27 mm diameter spot. The photon flux achieved with this setup is ~900 $\mu mol \cdot m^{-2} \cdot s^{-1}$ at the peak wavelength of the filter. Analysis of the UV/Vis spectra to deconvolute the contributions of the different components was performed by using the software package *ae*.[2] Fluorescence emission spectra were recorded on a NanoLog HORIBA Jobin-Yvon spectrophotometer (HORIBA Scientific, Japan). The excitation wavelength was chosen based on the dye used: 520 nm for direct excitation of Cy3, and 620 nm for excitation of Cy5. Generally, 2 and 5 nm slit widths of the excitation and emission monochromator were used, respectively. The photomultiplier tube was adjusted to avoid signal saturation of the detector (750 V). Emission spectra were recorded collecting data with 1 nm spacing, and with an integration time of 0.1 s per data point. Emission kinetics were recorded by continuous excitation of the dye with a suitable wavelength, and the emission was observed with a 0.5 s integration time per point. Data points were collected every 1 s, for at least 400 s per sample. The power of the excitation beam was modulated by using neutral density (ND) gray filters to attenuate the light reaching the cuvette. The beam at the sample is 7 mm × 2 mm, and it almost completely illuminates the sample in a 100 µl cuvette with a 10 mm x 2mm window, this ensures a homogeneous sample exposure to light. The temperature was controlled with an external water bath and it was kept constant at 20 ºC throughout all the experiments. Data were corrected for lamp intensity fluctuations by monitoring the power of the excitation light with the built-in detector of the NanoLog spectrophotometer. Energy transfer efficiencies were calculated from the emission spectra as follows:

$$E = 1 - \frac{I_{DA} A_D}{I_D A_{DA}}$$

Where I_D and A_D are, respectively, the intensity emission and the absorbance of the donor only sample, and I_{DA} and A_{DA} are the intensity emission and the absorbance of the donor in the presence of the acceptor.

The time traces measured under continuous illumination were normalized dividing the data by the emission at $t = 0$.

Time Correlated Single Photon Counting

Time Correlated Single Photon Counting (TCSPC) experiments were performed on a custom built spectrometer as previously described.[3] Briefly, the excitation was provided by a supercontinuum laser (Fianium SC450) with a repetition rate set to 20 MHz. The excitation wavelength was selected by using an Acousto-Optical Tunable Filter (Fianium AOTF) to obtain either 520 or 620 nm excitation light. To increase the illumination area in the sample during the experiment, the illumination beam was used collimated, as obtained after the AOTF, with a ~2 mm diameter. The sample was pipetted into a 45 µl cuvette with a 10 mm × 2 mm window, and sealed to avoid evaporation. The temperature was controlled by using an external water bath set at 20 ºC for all the measurements. Fluorescence emission was collected at a 90º angle, passed

through a polarizer set to 54.7° (magic angle), a double grating monochromator (Jobin-Yvon, Gemini-180), and focused onto a microchannel plate photomultiplier tube (Hamamatsu R3809U-50). Data collection was performed using a Becker-Hickl SPC830 counting card. The typical instrument response function showed a full width half maximum of ~60 ps, as measured by using a scattering solution. Data were fitted with the DecayFit software package.[4] The fitting function used for the data is of the form:

$$I(t) = \sum_i a_i e^{-\frac{t}{\tau_i}}$$

Where a_i is the pre-exponential factor accounting for the amplitude of each lifetime component τ_i. The average lifetime used to calculate the energy transfer rate was calculated according to:

$$\tau_{avg} = \sum_i a_i \tau_i$$

The average lifetimes were used for the calculations of the energy transfer efficiencies as follows:

$$E = 1 - \frac{\tau_{DA,avg}}{\tau_{D,avg}}$$

Where $\tau_{D,avg}$ and $\tau_{DA,avg}$ are the lifetimes of the donor in the absence and in the presence of the acceptor, respectively.

Supplementary Results/Discussions

OCP-St1 Purification

Anion exchange chromatography allowed the separation of the three components present after conjugating the protein to DNA: OCP, OCP-St1, and unreacted St1. The elution gradient (dashed line in Figure 1B) separates of the unmodified protein (peak 1), which elutes at 217 mM NaCl, from the protein-DNA conjugate (peak 2), which elutes at 405 mM NaCl. The unreacted DNA is also removed from the mixture, and it elutes at a later time at 446 mM NaCl (peak 3). The co-presence of protein and DNA is identified by the absorbance of OCP at 495 nm, and by an increase of the absorbance at 260 nm, with respect to unmodified OCP, due to the presence of the DNA strand. The UV/Vis spectrum suggested that the DNA to protein ratio for the purified sample was ~1.08 : 1. The product appears as a single band in gel electrophoresis (Figure S2) after staining with SybrGold for presence of DNA, and silver staining shows a clear major protein band that overlaps with the aforementioned DNA-containing band.

Assembly of OCP-3arm DNA-dyes complex and characterization

To form the 3arm DNA structure on the OCP, a stoichiometric amount of the other two DNA strands was mixed with OCP-St1. For thermal annealing a cooling ramp starting from 35 ºC was used. The formation of the final product was verified by both gel electrophoresis (Figure S2), and size exclusion chromatography (Figure S1D). The OCP-3arm elutes from the gel filtration column at a smaller retention volume compared to OCP-St1 (Figure S1B, S1C, and S1D). A shift

between the two samples is also visible on the gel in Figure S2, however it is less pronounced than what is observed with chromatography. Size exclusion chromatography was used to purify the assembled samples, in order to remove unassembled single stranded DNA, eluting at larger retention volume. The data presented show the successful assembly and purification of a 3arm DNA assembly on OCP: the gel, combined with the size exclusion chromatography, confirm that the 3arm junction is formed. The shift in retention volume during gel filtration indicates a larger hydrodynamic radius of the OCP-3arm compared to OCP-St1, and this is in line with the presence of a bulkier, three dimensional DNA structure, compared to single stranded DNA. Also, the presence of OCP on the 3arm junction considerably shifts the elution of the DNA nanostructure toward smaller retention volumes (Figure S1A, S1C, and S1D).

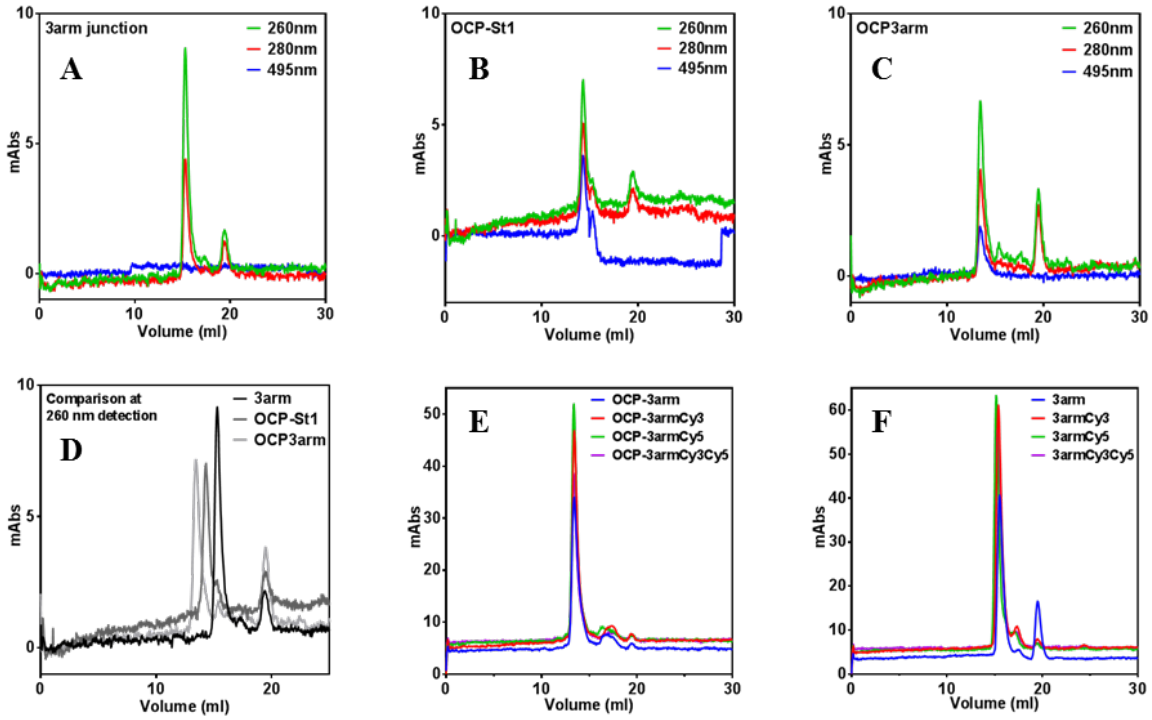

Figure S 1. Results from size exclusion chromatography runs on various samples: panels A) through D) show analytical runs on 3arm, OCP-St1 and OCP3arm samples. Panels E) and F) show the preparatory runs to purify the 3arm and OCP3arm sample used for the subsequent characterization experiments. In panels A), B), and C) the elution profile at 3 wavelengths is shown. The wavelengths chosen are 260, 280, 495 nm, and they are used to monitor the characteristic absorption of DNA, protein and carotenoid, respectively. In panels D), E), and F), for simplicity only the absorbance at 260 nm is shown to compare the elution profile of the different samples.

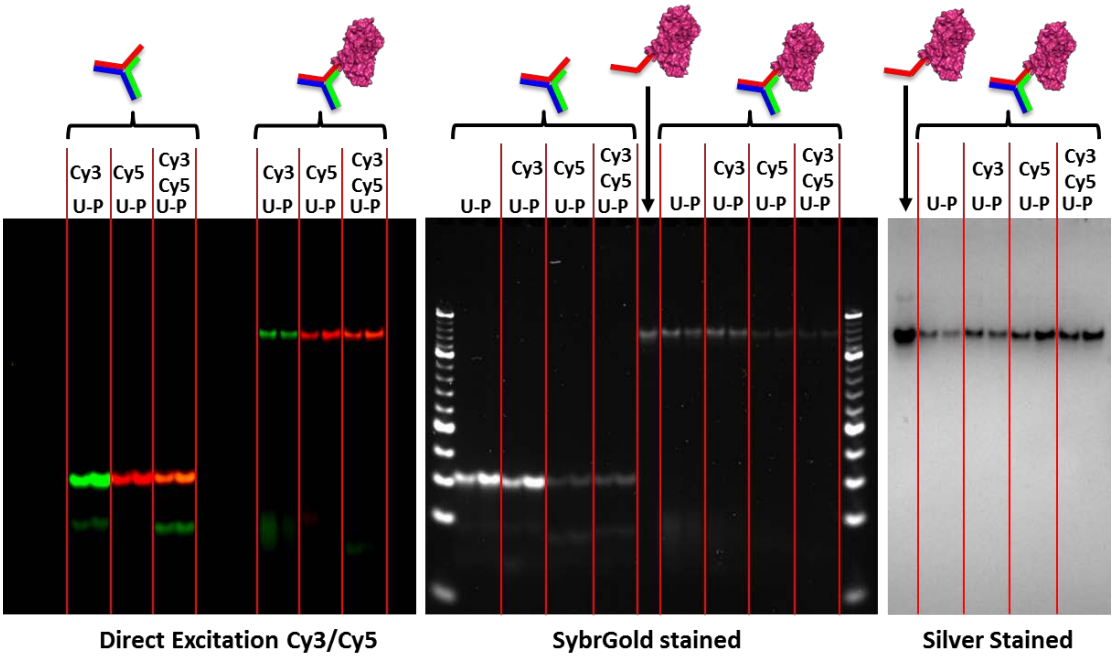

Figure S 2. Gel electrophoresis analysis results on OCP-St1, 3arm and OCP3arm samples. The sample loaded is indicated by the schematic cartoon depicted above the gels. The samples are grouped based on the version of label attached to them. Each couple of lanes was either loaded with the sample before (U = unpurified) or after (P = purified) size exclusion chromatography. Left to right, the images were obtained, respectively: by direct excitation of Cy3 or Cy5 and imaging of their emission on a Typhoon scanner, by staining with SybrGold to visualize also the unlabeled nucleic acid, and by using silver staining to visualize the proteins in the bands.

A comparison of the samples before and after the purification is presented in Figure S2. The overall amount of single stranded DNA, based on the intensities of the bands, is very low compared to the amount of formed products. It is also clear that, especially for the OCP-3arm samples, after gel filtration the amount of free, unassembled strands becomes negligible. The co-migration of protein, DNA and dyes (Cy3, Cy5 or both) in the polyacrylamide native gel (Figure S2) also confirms that the DNA strands carrying the labels are correctly incorporated. The UV/Vis spectroscopy data show that the OCP-3arm complexes constructed have a stoichiometry close to 1:1 for all the components involved, highlighting the advantage of using DNA as a scaffold. The slight defect of DNA or dyes observed in the complex compared to OCP (Figure S3) may be due to incomplete assembly, or inaccuracies in the extinction coefficient used to calculate the concentration of these components: after the assembly of the 3arm junction, changes in the environment surrounding those elements could affect their absorption properties. However, it is important to notice that in all cases there is no more than one dye, or dye couple, per protein and this allows to analyze the data in a straightforward manner.

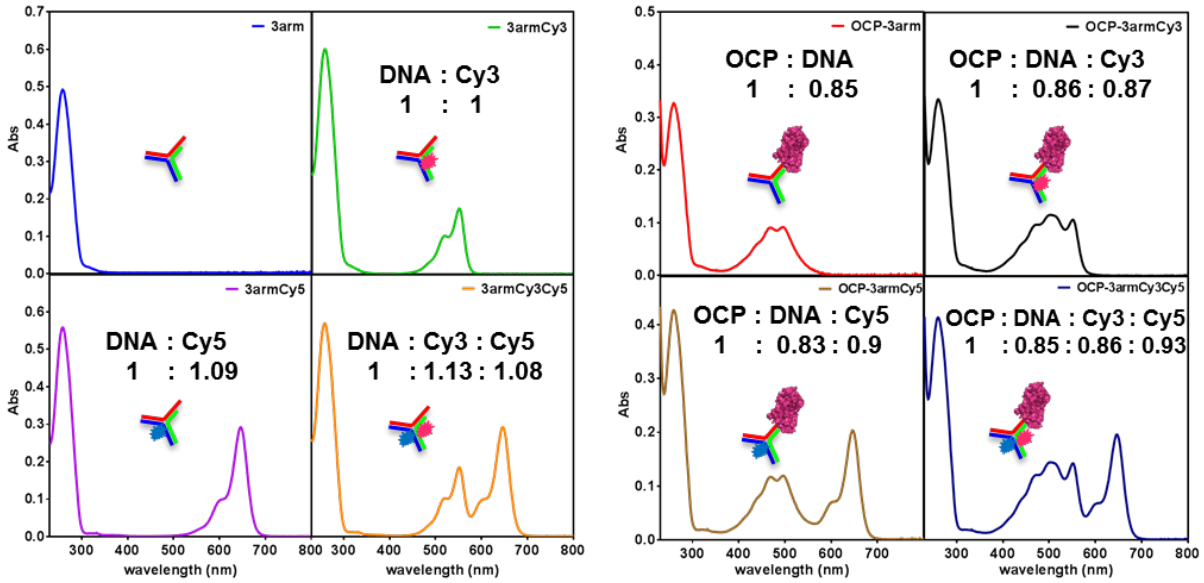

Figure S 3. UV/Vis spectra of the samples obtained after size exclusion chromatography. The left 4 panels are the spectra of the 3arm constructs showing the features of DNA (260 nm) and the two dyes (Cy3, 552 nm, and Cy5, 647 nm). The right 4 panels show the spectra of the OCP3arm constructs with spectral signatures of DNA (260 nm), Cy3 (552 nm), Cy5 (647 nm), and OCP (469 and 495 nm). The ratio between the components are indicate on each spectrum. Spectral overlaps of different components in the 350 – 750 nm region were deconvolved for calculations of the concentration

Test of the photoconversion activity of the DNA-conjugated OCP is presented in Figure S4.

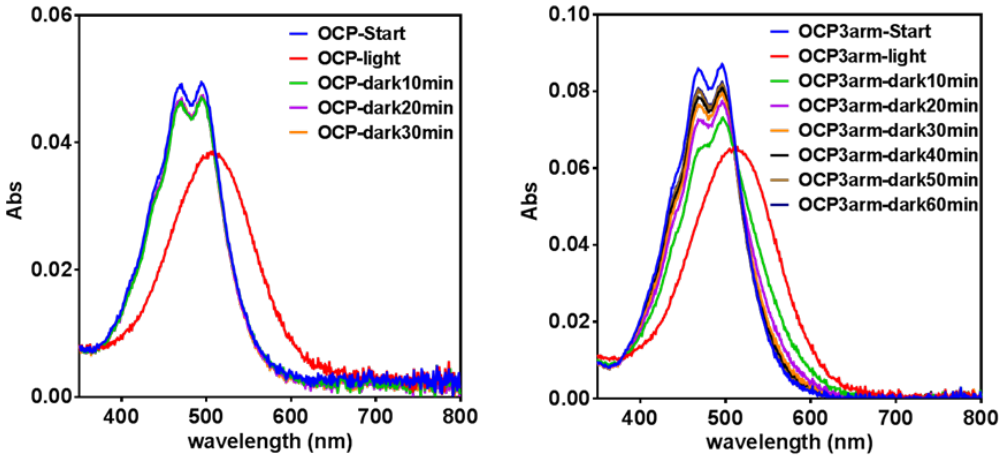

Figure S 4. Photoconversion of OCP and OCP3arm. Left: OCP in the "OCP3arm buffer" to test the effect of the buffer on the photoconversion of the protein. After light exposure, the activated (red) protein was allowed to relax in the dark and a spectrum was taken every 10 minutes. It is quite clear that after 10 minutes the protein was already converted back to its inactive form. Right: the same test was repeated on the OCP3arm sample to verify its ability to convert between the two states. The data show that the recovery from activated state of OCP in the OCP3arm sample is slower than for OCP alone: it takes approximately 40-50 minutes before the spectrum recovers the shape of the sample before illumination.

Energy Transfer Rate Calculations

For the energy transfer calculations in the OCP^{O}-3arm-Cy3, and OCP^{O}-3arm-Cy3-Cy5 samples, an excess of FRP was used to "hold" the protein in its inactive, orange, state. The effect of FRP

on the OCP-3arm construct was evaluated by adding it to a sample of OCPR-3arm that was previously photo-converted by exposure to ~900 μmol·m^{-2}·s^{-1} photons for 5 minutes. The results are presented in Figure S5: the presence of FRP speeds up the recovery of the OCP^{O} spectral features such that it is almost immediate upon adding it to the sample. The value of k_1 was obtained by using the data of OCP-3arm-Cy3 measured in presence of an excess of FRP, k_2 was calculated from the data measured at the highest power value for the OCP-3arm-Cy3 sample, and k_3 is from measurements of the 3arm-Cy3-Cy5 sample in the absence of OCP. Though the FRET efficiencies were determined by using steady state and TCSCP measurements, only the latter were used due to the intrinsic character of lifetime compared to intensity, making it a more reliable indicator for FRET calculations.[5]

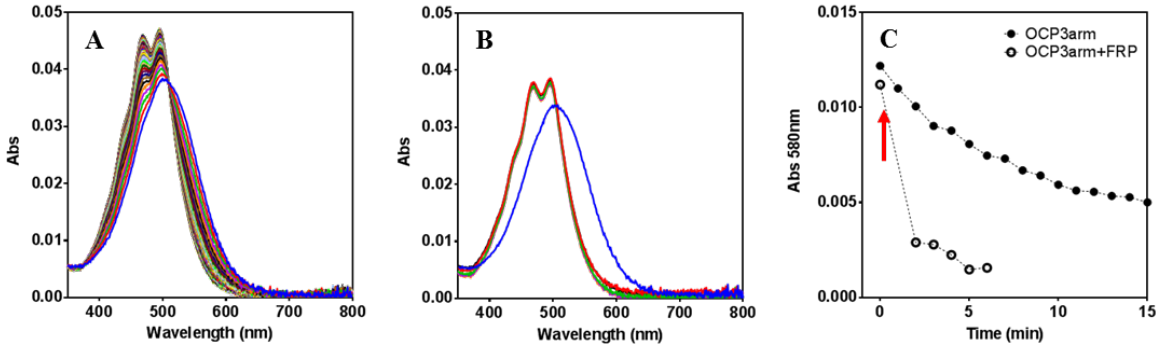

Figure S 5. Effect of FRP on the photoconversion *active* -> *inactive* of the OCP3arm sample. A) After illumination with blue-green light (380-480 nm), the OCP3arm sample (blue trace) was left in the dark and an absorption spectrum was taken every 1 minute. B) The same experiment reported in panel A was performed in presence of a 1-fold excess of FRP to OCP3arm. C) The absorbance at 580 nm from the plots in panel A and B are plotted as a function of time to highlight the difference in recovery between the OCP3arm and the OCP3arm+FRP samples. The red arrow indicates the time stamp of the addition of FRP to the sample.

Emission of Cy5 in OCP-3arm-Cy3-Cy5 and OCP-3arm-Cy5

The main focus of this work is the investigation of the influence of OCP on the dye Cy3, connected in close proximity to the carotenoid by the 3arm junction. The dye Cy5, being the acceptor of the antenna system, was positioned further away from the protein, to decrease direct energy transfer with the carotenoid. However, during TCSPC measurements on Cy5 in the OCP-3arm-Cy3-Cy5 complex, a small decrease of the lifetime of Cy5 is observed at higher excitation intensities (Figure S6B).

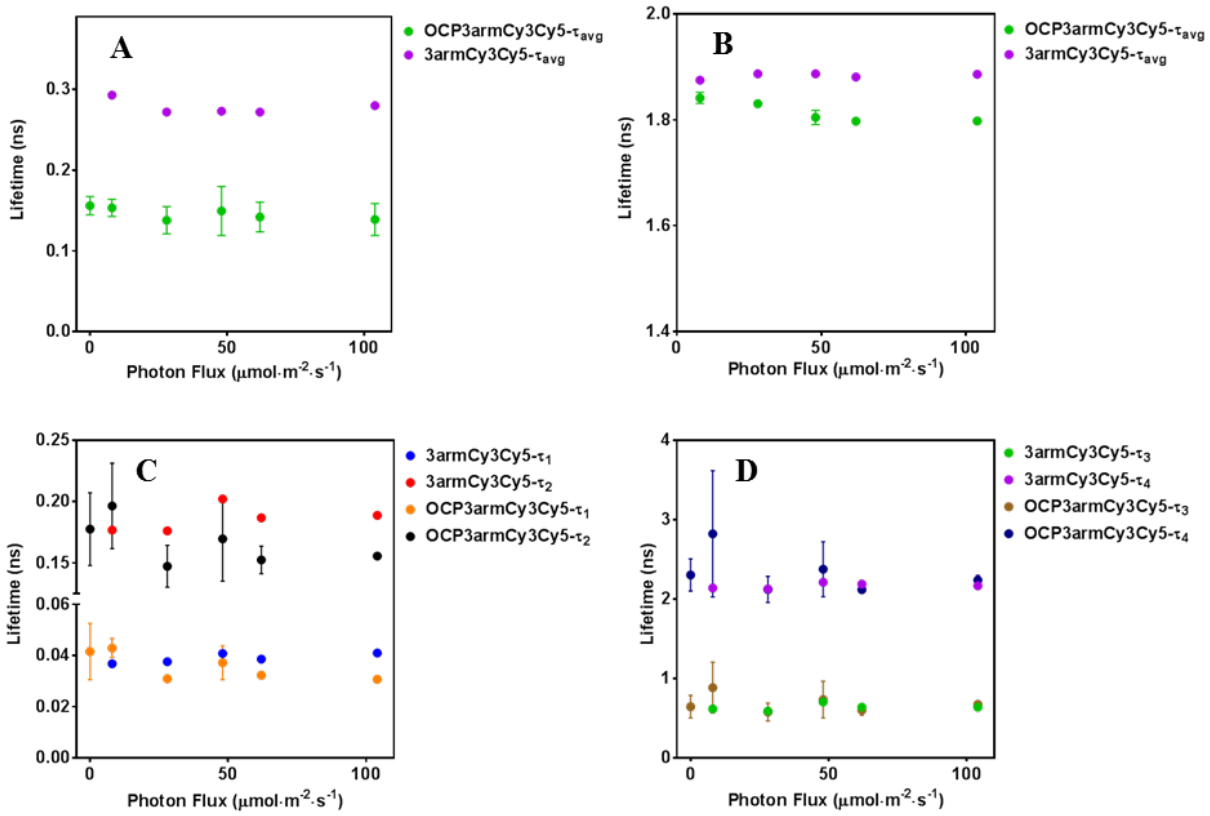

Figure S 6. A) average lifetime values of 3armCy3Cy5 and OCP3armCy3Cy5 samples as a function of excitation intensity. The samples were excited at 520 nm and the fluorescence at 566 nm, corresponding to the emission of Cy3, was detected. The value at a photon flux of 0 mmol·m^{-2}·s^{-1} is obtained by using an excess of FRP in the solution containing OCP3armCy3Cy5, and measuring at low power intensity. B) Average lifetime values of Cy5 on the 3armCy3Cy5 and OCP3armCy3Cy5 samples upon excitation at 520 nm and detection at 662 nm. C) Lifetime components of Cy3 in the 3armCy3Cy5 and OCP3armCy3Cy5 structures. The two shortest lifetimes are reported here as a function of illumination intensity. It is noticeable how the lifetime values of Cy3 in OCP3armCy3Cy5 become shorter than what observed for 3armCy3Cy5 at photon fluxes higher than 8 mmol·m^{-2}·s^{-1}. D) Here the two longest lifetime components of Cy3 for the Cy3Cy5 samples are shown. It is possible to see in this case that the values for the 3arm and the OCP3arm samples are very similar to each other through the whole range of illumination intensities used.

As shown in the Appendix below, the presence of three components in the FRET system does not influence directly the emission decay of the acceptor dye, unless energy transfer between the dye and the OCP occurs. By taking a closer look at the absorption and emission spectra of OCP^{R} and Cy5, respectively (Figure S7) it appears that there is a small overlap in the 600 – 650 nm region. This overlap may account for the decrease of the Cy5 lifetime at higher excitation intensities: the photoconversion of OCP^{O} to OCP^{R} will give rise to energy transfer from the dye to the carotenoid. This effect is considerably lower than what we observe for Cy3: the lifetime of Cy5 decreases ~2.5% versus the ~40% decrease observed for Cy3. Furthermore, we think that the contribution of this effect to the observed decrease of emission of Cy5 as seen in Figure 3B is negligible compared to the diminished energy transfer from Cy3 to Cy5 due to the competition with OCP^{R}.

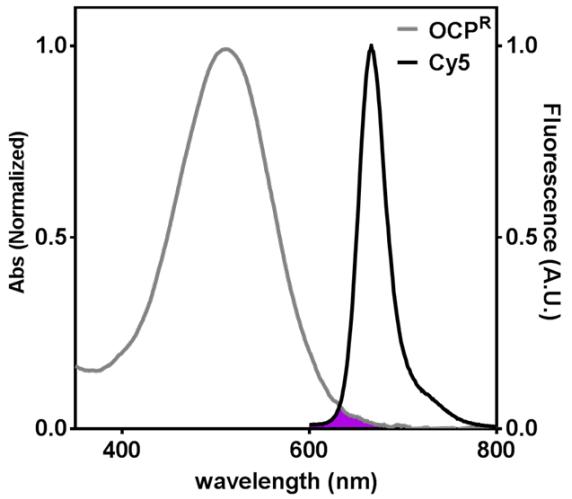

Figure S 7. Spectral overlap (purple area) between the absorption of OCP^R (gray line) and emission of Cy5 (black line), the spectra were normalized at their maximum for comparison.

It is noteworthy that the activation of OCP^R that gives rise to quenching of Cy5 occurs in the sample OCP-3arm-Cy3-Cy5. Figure S9B shows the results from TCSPC measurements on the OCP-3arm-Cy5 sample either with excitation at 620 nm, or with double excitation at 620 and 520 nm. The former should not result in activation of OCP, 620 nm being outside of the absorption band of the carotenoid, whereas the latter should indeed activate the protein as observed with other samples: as shown in Figure S9B, no change in the lifetime is observed compared to the reference sample 3arm-Cy5. A possible explanation for the difference between the effects of green light (520 nm) on OCP-3arm-Cy3-Cy5 and on OCP-3arm-Cy5 may lie in the presence of Cy3 that increases the absorption cross-section of the complex at 520 nm, compared to OCP alone. The energy transfer Cy3- >OCP may contribute to the photo-activation of OCP and its transition to the OCP^R form at lower photon fluxes than OCP alone.

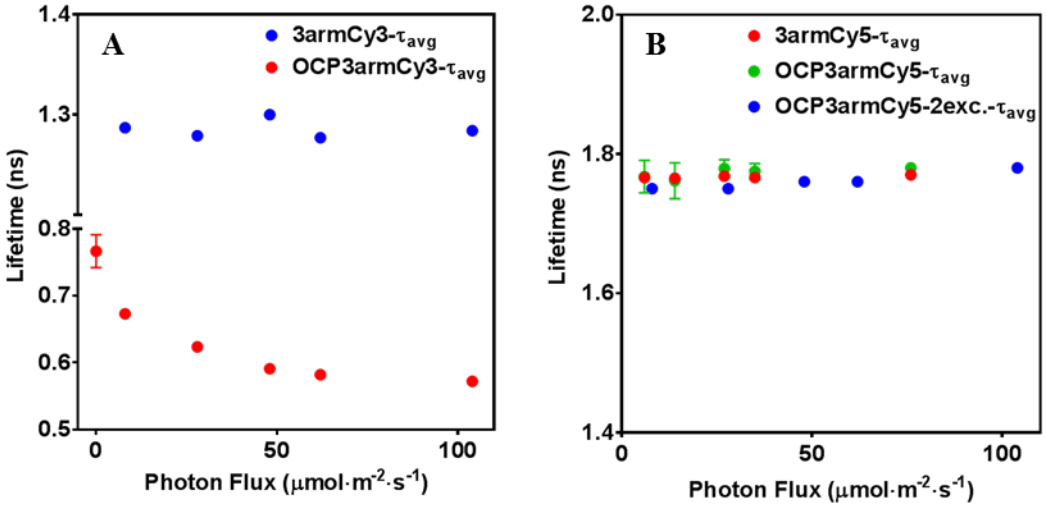

Figure S 8. Average lifetimes of singly labeled constructs. The lifetimes were extracted from the analysis of the TCSPC histograms as described in the text. A) Average lifetime of Cy3 labeled samples. Excitation at 520 nm, detection at 566 nm. The value at a photon flux of 0 mmol·m^{-2}·s^{-1} is obtained by using an excess of FRP in the solution, and measuring at low excitation power. B) Average lifetime of Cy5 labeled construct. Excitation at 620 nm, detection at 662 nm. The sample OCP3armCy5-2exc. was excited simultaneously at 520 and 620 nm. The excitation at 620 nm was kept fixed and the TCSPC decays were recorded at different intensities of 520 nm excitation.

Appendix Calculations

Modeling of the TCSPC decays in the OCP-3arm-Cy3-Cy5 system

The modeling of the TCSPC decays of the OCP-3arm-Cy3-Cy5 system was done to check if the decrease in the emission of the lifetime of Cy5 observed in Figure S6B was related to the presence of a second acceptor in the FRET system. The kinetic scheme of Figure4A was used as a reference, however the Cy5 -> OCP^R transfer was neglected. The scheme was also simplified by incorporating k_1 and k_2 together to take into account the equilibrium between the two species of OCP, the apparent transfer rate from Cy3 to OCPO and OCPR is indicated as:

$$k_1' = (1-\alpha)k_1 + \alpha k_2$$

The population of the excited state for the donor (Cy3) and the acceptor (Cy5) can be described by using the following system of coupled ODEs:

$$\frac{dD(t)}{dt} = -(k_D + k_1' + k_3)D(t)$$

$$\frac{dA(t)}{dt} = k_3 D(t) - k_A A(t)$$

With initial conditions: $D(0) = D_0$ and $A(0) = 0$. Solving the system to obtain the time dependent evolution of the populations of the excited states yields:

$$D(t) = D_0 e^{-(k_D + k_1' + k_3)t}$$

$$A(t) = \frac{D_0 k_3}{k_D + k_1' + k_3 - k_A}(e^{-k_A t} - e^{-(k_D + k_1' + k_3)t})$$

Where k_D and k_A are the decay rate transfer of donor and acceptor, respectively, and are equal to the inverse of their respective lifetime. The time evolution of the acceptor dye, Cy5, is indicated by *A(t)* and the equations is composed of a pre-exponential term and two exponential: a positive one associated with the decay, and a negative one that describes the rise due to the FRET from Cy3 to Cy5. It is clear from these equations that only the rise of *A(t)* should be influenced by the presence of the other acceptor, whereas the decay only depends on k_A.

Quenching of Cy3 and Cy5 under continuous illumination

By using the energy transfer rates obtained from the experiments, it is possible to model the quenching of Cy3 and Cy5 under continuous illumination conditions. We start by considering the photoconversion reaction of OCP:

$$OCP^O \underset{k_{-1}}{\overset{F\cdot\sigma}{\rightleftharpoons}} OCP^R$$

Where F is the incident photon flux on the sample, σ is the absorption cross section of the molecule, and k_{-1} is the light-independent back conversion rate constant of OCP. We can calculate the amount of OCP^R in the sample as:

$$OCP^R = \frac{F \cdot \sigma}{F \cdot \sigma + k_{-1}}$$

As a next step we define the apparent energy transfer rate k_1' in a sample that contains a mixture of OCP^O and OCP^R, as a function of k_1 and k_2 as presented in Figure 4:

$$k_1' = (1 - OCP^R) \cdot k_1 + OCP^R \cdot k_2$$

We define the emission of Cy3 similarly to a quantum yield:

$$EM_{Cy3} = \frac{\frac{1}{\tau_{Cy3}}}{k_1' + k_3 + \frac{1}{\tau_{Cy3}}}$$

Note that the above equation can be modified for a system where Cy5 is not present, by simply removing the term k_3.

In the case of Cy5, the emission intensity is proportional to the energy received from Cy3, and thus we can use the energy transfer efficiency, for simplicity, as a measure of the emission for our scope:

$$E_{Cy3\to Cy5} = \frac{k_3}{k_1' + k_3 + \frac{1}{\tau_{Cy3}}}$$

The emission of Cy3 and the energy efficiency transfer Cy3->Cy5 are both a function of illumination intensity flux (F), due to the definition of k_1' as a function of the fraction of OCP^R. To calculate the relative energy transfer efficiency as presented in Figure 2D and 3C, we use the following equations, as also defined in the main text:

$$relE_{Cy3}(F) = 1 - \frac{EM_{Cy3}(F)}{EM_{Cy3}(F=0)}$$

$$relE_{Cy5}(F) = \frac{E_{Cy3\to Cy5}(F)}{E_{Cy3\to Cy5}(F=0)}$$

Where EM_{Cy3} and $E_{Cy3->Cy5}$ stands for the observable I_{Cy3} and I_{Cy5} used in the main text.

To perform further calculations, the values of the parameters were chosen as follows:

a. The rate parameters k_1, k_2, and k_3 are presented in Figure 4B
b. The value of k_{-1} for the OCP-3arm system can be extracted from the data in Figure S5C (~0.2 s^{-1})
c. A value of σ~4×10^{-16} cm^2 for OCP was used at 497 nm
d. The experimental values of F used in this work are in the range from 1 to 100 μmol photons·m^2·s^{-1}.

By using these parameters it is possible to model the quenching of fluorescence by OCP in the OCP-3arm-Cy3 or in the OCP-3arm-Cy3-Cy5 systems for the continuous illumination experiments. The results are presented in Figure S9: the modeled quenching as a function of illumination intensity flux follows very closely the data presented in Figure 2D and Figure 3C.

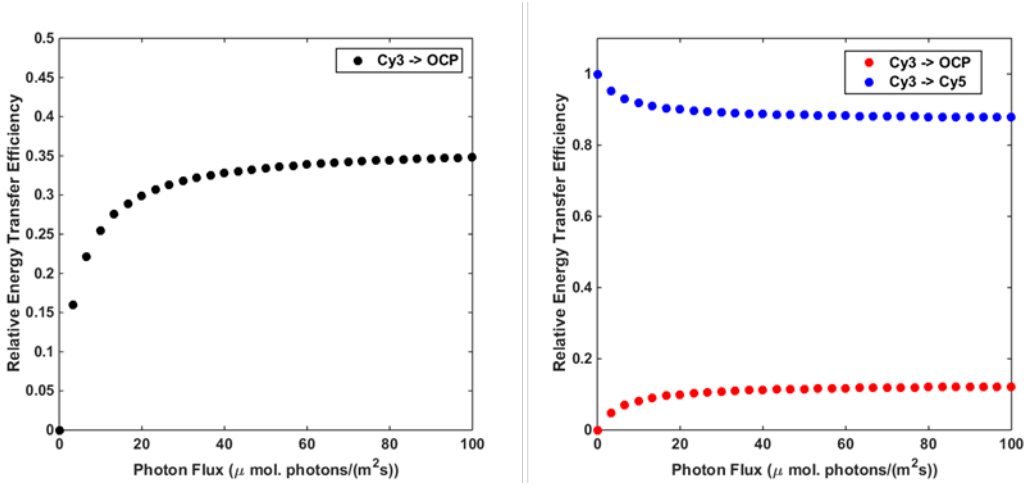

Figure S 9. Modeled relative energy transfer efficiency as a function of photon flux for the continuous illumination experiments. Left: Cy3 -> OCP transfer in the OCP-3arm-Cy3 system, based on the energy transfer rate parameters obtained from the

experiments. Right: Cy3 -> OCP and Cy3 -> Cy5 transfer in the OCP-3arm-Cy3-Cy5 system, based on the based on the energy transfer rate parameters obtained experimentally.

Supplementary Figures

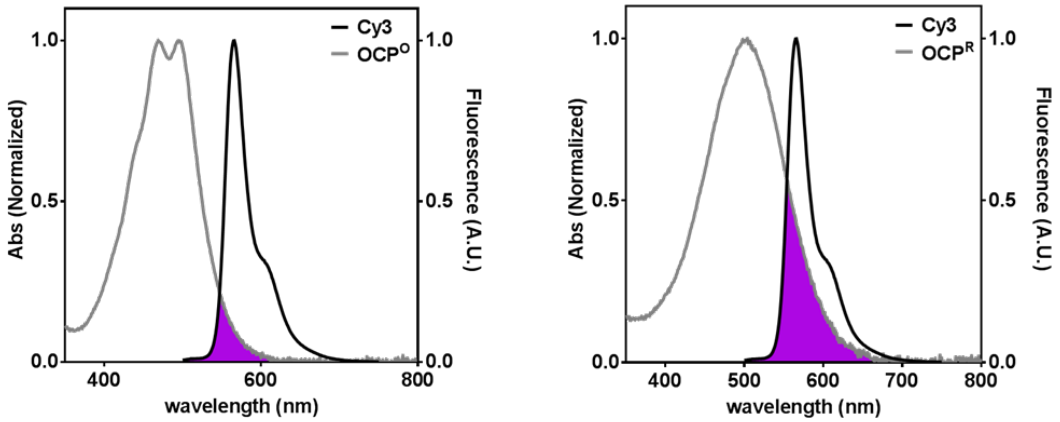

Figure S 10. Spectral overlap (purple area) between the absorption of OCP (gray line) and emission of Cy3 (black line) with OPC in the inactive (left panel) and active (right panel) state. The spectra were normalized at their maximum for comparison.

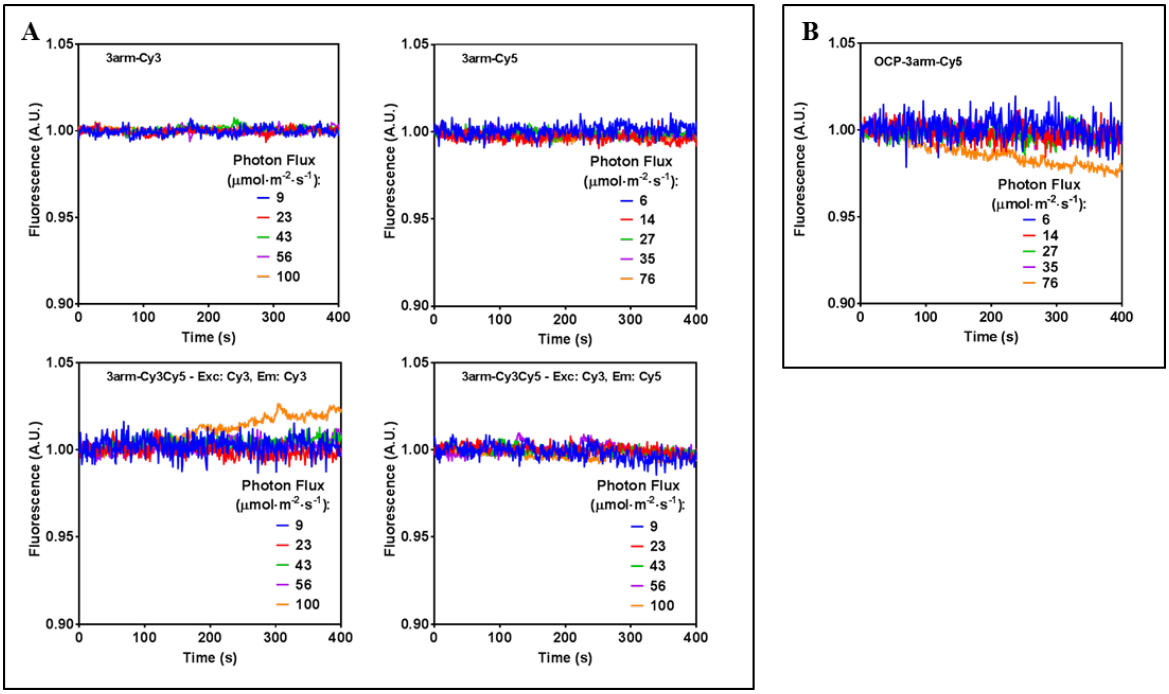

Figure S 11. A) Fluorescence intensity of the 3 configurations of the 3arm labeled samples under continuous illumination. Top left: excitation of 3armCy3 at 520 nm and detection at 566 nm. Top right: excitation of 3armCy5 at 620nm and detection of the emission at 662 nm. Bottom left: 3armCy3Cy5 was excited at 520 nm, and the emission at 566 nm was recorded. Bottom right: emission of 3armCy3Cy5 at 662 nm upon excitation at 520 nm at various intensities. B) Steady state fluorescence emission of OCP3armCy5 excited at 620 nm and detected at 662 nm at the intensities indicated on the plot.

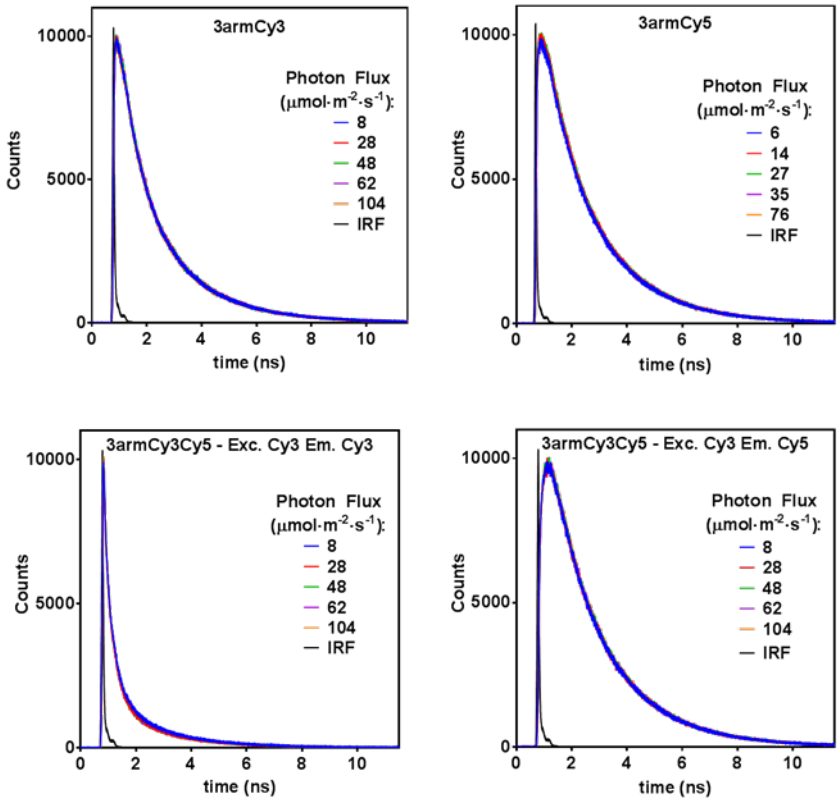

Figure S 12. TCSPC data illustrates fluorescence intensity decay of the 3arm samples in different configurations. The sample name is indicated on the plot. Top left: excitation at 520 nm, detection at 566 nm. Top right: excitation at 620 nm, detection at 662 nm. Bottom left: excitation at 520 nm, detection at 566 nm. Bottom right: excitation at 520 nm, detection at 662 nm. In all the plots the instrument response function (IRF) is plotted along with the data.

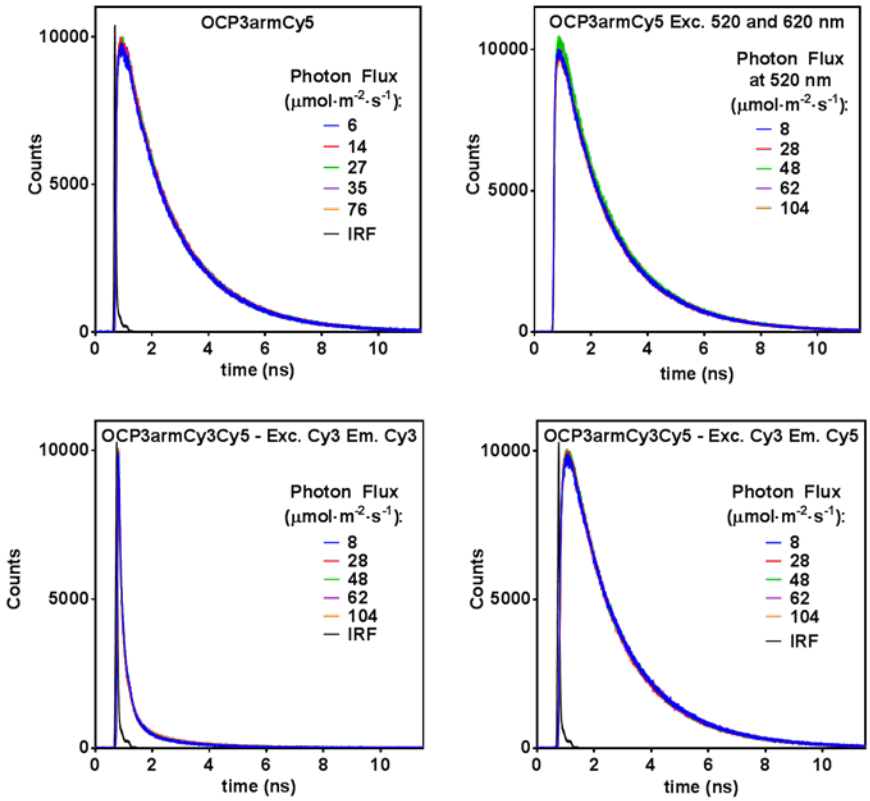

Figure S 13. TCSPC data for fluorescence intensity decay of the OCP3arm samples with different dyes configuration. The sample name is indicated on each panel. Top left: excitation at 620 nm, detection at 662 nm. Top right: excitation of the sample with two overlaid beams at 520 and 620 nm, to excite OCP and Cy5, respectively. The signal was detected at 662 nm. Bottom left: excitation at 520 nm and detection at 566 nm. Bottom right: excitation at 520 nm and detection at 662 nm. In all the plots the instrument response function (IRF, black line) is plotted along with the data.

Supplementary Tables

Strand Full Name	Strand Short Name	Sequence 5' -> 3' (with IDT modifications notation)	Modifications
3arm-1 3'SH 5'biotin	St1	/5Biosg/TCG CTA GGA ACG GAT TTT/3ThioMC3-D/	3' – C_3 linker-Thiol 5'-biotin
3arm-2	St2	ATC CGT TGA TGT AGC G	/
3arm-3	St3	CGC TAC ATC ATC CTA GCG A	/
3arm-2-5'-Cy3	St2Cy3	ATC CGT TGA TGT AGC G	5'-Cy3
3arm-3-iCy5(10)	St3Cy5	CGC TAC ATC A/iCy5/TC CTA GCG A	Internal Cy5

Table S 1. DNA strand used to build the 3arm junction. Strands St2 and St3 were obtained with or without dye modification, to allow for the assembly of different structures. Strand St1 was originally designed with a biotin modification to use a biotin-streptavidin purification approach. This method was not used for the present work, however the strand was used as originally ordered.

Sample	FRET (%) (steady state)	FRET (%) (TCSPC)	Acceptor
3armCy3Cy5	85 (±2)	78	Cy5
OCP3armCy3	60 (±3)	40	OCP^O
OCP3armCy3	77	55	OCP^R
OCP3armCy3Cy5	92 (±0.01)	88	OCP^O,Cy5
OCP3armCy3Cy5	94	89	OCP^R,Cy5

Table S 2. FRET efficiencies from Cy3 to either OCP^O, OCP^R, or Cy5 as calculated from the experimental data. The steady state and the TCSPC values are reported here for comparison.

Lifetime (ns) Amplitudes	3armCy3 (em: 566 nm)				
	6 μW	**20 μW**	**35 μW**	**45 μW**	**75 μW**
τ_1	0.2209	0.1907	0.2505	0.1875	0.2234
a_1	0.1574	0.1485	0.152	0.1444	0.1575
τ_2	0.8801	0.8495	0.8692	0.8352	0.8624
a_2	0.4506	0.4478	0.4418	0.4479	0.4386
τ_3	2.1828	2.156	2.1603	2.1484	2.1548
a_3	0.392	0.4037	0.4062	0.4076	0.404
τ_{avg}	**1.287**	**1.279**	**1.300**	**1.277**	**1.284**

Table S 3. Fluorescence decay lifetimes and their amplitudes obtained for a 3-exponential fitting of the TCSPC data from 3armCy3 sample at different excitation intensities. Excitation at 520 nm, and detection at 566 nm. The average lifetime, calculated as indicated in the methods, is reported in the bottom row.

Lifetime (ns) Amplitudes	3armCy3Cy5 (em: 566 nm)					3armCy3Cy5 (em: 662 nm)				
	6 μW	**20 μW**	**35 μW**	**45 μW**	**75 μW**	**6 μW**	**20 μW**	**35 μW**	**45 μW**	**75 μW**
τ_1	0.0368	0.0376	0.0408	0.0386	0.041	0.123	0.1162	0.1207	0.1247	0.1188
a_1	0.4709	0.4828	0.517	0.4973	0.4912	-0.5567	-0.6131	-0.6836	-0.6286	-0.6671
τ_2	0.1769	0.1762	0.2022	0.1868	0.1888	1.2211	1.33	1.3974	1.3238	1.3547
a_2	0.35	0.3458	0.3397	0.3445	0.3452	0.392	0.5075	0.6925	0.5511	0.5763
τ_3	0.616	0.5875	0.7032	0.6381	0.6375	2.1344	2.1875	2.2265	2.1881	2.1929
a_3	0.1112	0.1115	0.0888	0.1017	0.1042	0.9871	0.9407	0.9999	0.9998	0.9997
τ_4	2.1391	2.1256	2.2116	2.1867	2.1667	/	/	/	/	/
a_4	0.068	0.06	0.0545	0.0565	0.0594	/	/	/	/	/
τ_{avg}	**0.293**	**0.272**	**0.273**	**0.272**	**0.280**	**1.875**	**1.887**	**1.887**	**1.881**	**1.886**

Table S 4. Fluorescence decay lifetimes and amplitudes obtained for the TCSPC experiments on 3armCy3Cy5 sample at different excitation intensities. Excitation at 520 nm, detection at 566 nm (left side of the table), and detection at 662 nm (right side of the table). The average lifetime, calculated as indicated in the methods, is reported in the bottom row. The negative amplitudes for the lifetimes measured at 662 nm are associated with the rise of the fluorescence decay due to FRET from the donor dye. The average lifetime reported in this case was calculated without taking the rise component into account.

Lifetime (ns) Amplitudes	OCP3armCy3 (em: 566 nm)					
	6 μW + FRP	**6 μW**	**20 μW**	**35 μW**	**45 μW**	**75 μW**
τ_1	0.1873	0.1441	0.1324	0.1094	0.1083	0.1089
a_1	0.3813	0.4022	0.4796	0.4961	0.5138	0.5268
τ_2	0.7493	0.6666	0.6746	0.6132	0.6173	0.6122
a_2	0.4612	0.4353	0.3721	0.3519	0.3375	0.3256
τ_3	2.1109	1.9977	2.1087	2.0872	2.1158	2.1457
a_3	0.1575	0.1625	0.1483	0.1521	0.1486	0.1476
τ_{avg}	**0.749**	**0.673**	**0.627**	**0.588**	**0.578**	**0.573**

Table S 5. Fluorescence decay lifetimes and their amplitudes obtained for the TCSPC experiments on OCP3armCy3 at different excitation intensities. The excitation used was 520 nm, and the fluorescence was detected at 566 nm. The average lifetime, calculated as indicated in the methods, is reported in the bottom row.

Lifetime (ns) Amplitudes	OCP3armCy3Cy5 (em: 566 nm)						OCP3armCy3Cy5 (em: 662 nm)				
	6 μW + FRP	**6 μW**	**20 μW**	**35 μW**	**45 μW**	**75 μW**	**6 μW**	**20 μW**	**35 μW**	**45 μW**	**75 μW**
τ_1	0.0493	0.0403	0.0299	0.0325	0.0322	0.0317	0.0817	0.0664	0.0709	0.0598	0.0755
a_1	0.6258	0.6332	0.6355	0.6718	0.6725	0.7062	-0.4563	-0.6374	-0.4627	-0.5336	-0.4721
τ_2	0.1986	0.1719	0.1353	0.1453	0.1446	0.1552	1.0728	1.3179	1.0621	1.0873	1.2094
a_2	0.3092	0.2992	0.2834	0.2566	0.2535	0.2324	0.2997	0.7552	0.3722	0.3808	0.6397
τ_3	0.7447	0.6581	0.4975	0.5688	0.5552	0.6449	2.0775	2.231	2.0696	2.0696	2.1664
a_3	0.0512	0.0523	0.062	0.0536	0.0549	0.0439	0.9356	0.9625	0.9939	0.9806	0.9982
τ_4	2.4476	2.2587	2.0039	2.1304	2.1282	2.1952	/	/	/	/	/
a_4	0.0138	0.0154	0.0191	0.018	0.0191	0.0175	/	/	/	/	/
τ_{avg}	**0.164**	**0.146**	**0.126**	**0.128**	**0.129**	**0.125**	**1.834**	**1.830**	**1.795**	**1.795**	**1.793**

Table S 6. Fluorescence decay lifetimes and their amplitudes obtained for the TCSPC experiments on OCP3armCy3Cy5 sample at different excitation intensities. Excitation at 520 nm, detection at 566 nm (left side of the table), and detection at 662 nm (right side of the table). The average lifetime, calculated as indicated in the methods, is reported in the bottom row. The negative amplitudes for the lifetimes measured at 662 nm are associated with the rise of the fluorescence decay due to FRET from the donor dye. The average lifetime reported in this case was calculated without taking the rise component into account.

Lifetime (ns) Amplitudes	3armCy5 (em: 662 nm)				
	3.5 μW	**8.5 μW**	**16.5 μW**	**21 μW**	**46 μW**
τ_1	0.943	0.944	0.980	0.952	1.002
a_1	0.264	0.268	0.287	0.268	0.294
τ_2	2.060	2.066	2.085	2.064	2.089
a_2	0.737	0.732	0.713	0.732	0.706
τ_{avg}	**1.766**	**1.765**	**1.768**	**1.766**	**1.770**

Table S 7. Fluorescence decay lifetimes and their amplitudes obtained for the TCSPC experiments on 3armCy5 at different excitation intensities. Excitation at 620 nm, and detection at 662 nm. The average lifetime, calculated as explained in the methods, is reported in the bottom row.

Lifetime (ns) Amplitudes	OCP3armCy5 (em: 662 nm)					OCP3armCy5 (ex: 520 nm and 620 nm; em: 662 nm)				
	3.5 μW	**8.5 μW**	**16.5 μW**	**21 μW**	**46 μW**	**6 μW**	**20 μW**	**35 μW**	**45 μW**	**75 μW**
τ_1	0.943	0.944	0.980	0.952	1.002	1.9735	1.9677	1.9577	1.9783	1.9907
a_1	0.264	0.268	0.287	0.268	0.294	0.8157	0.8188	0.8308	0.8107	0.7975
τ_2	2.060	2.066	2.085	2.064	2.089	0.7836	0.7707	0.7688	0.8371	0.9392
a_2	0.737	0.732	0.713	0.732	0.706	0.1843	0.1812	0.1692	0.1893	0.2025
τ_{avg}	**1.766**	**1.765**	**1.768**	**1.766**	**1.770**	**1.754**	**1.751**	**1.757**	**1.762**	**1.778**

Table S 8. Fluorescence decay lifetimes and their amplitudes obtained for the TCSPC experiments on OCP3armCy5 at different excitation intensities. Excitation at 620 nm, and detection at 662 nm (left side). The right side of the table reports the lifetime components obtained for a double wavelength excitation experiment where 520 and 620 nm beam were used to illuminate the sample. The power of the 620 nm beam was kept constant, whereas the illumination at 520 nm was changed (indicated in the column header). The average lifetime, calculated as indicated in the methods, is reported in the bottom row.

Supplementary References

1. Zhang, H.; Liu, H.; Niedzwiedzki, D. M.; Prado, M.; Jiang, J.; Gross, M. L.; Blankenship, R. E. *Biochemistry-Us* **2014,** 53, (1), 13-19.
2. *a|e - UV-Vis-IR Spectral Software 2.2* **FluorTools,** www.fluortools.com.
3. Dutta, P. K.; Levenberg, S.; Loskutov, A.; Jun, D.; Saer, R.; Beatty, J. T.; Lin, S.; Liu, Y.; Woodbury, N. W.; Yan, H. *J Am Chem Soc* **2014,** 136, (47), 16618-16625.
4. *DecayFit - Fluorescence Decay Analysis Software 1.3* **FluorTools,** www.fluortools.com.
5. Berezin, M. Y.; Achilefu, S. *Chem Rev* **2010,** 110, (5), 2641-2684.